Open Access

Catalysis Research

LIDSEN Publishing Inc.

Research Article

Synthesis of NaA Zeolite: Conventional Route and Green Route

Antusia dos Santos Barbosa [†], Meiry Gláucia Freire Rodrigues [†, *]

Universidade Federal de Campina Grande, Unidade Acadêmica de Engenharia Química, 58109-970 Campina Grande - PB, Brazil; E-Mails: antusiasb@hotmail.com; meiry.freire@eq.ufcg.edu.br

† These authors contributed equally to this work.

* **Correspondence:** Meiry Gláucia Freire Rodrigues; E-Mail: meiry.freire@eq.ufcg.edu.br

Academic Editors: Angela Martins and Antonio Chica

Special Issue: Zeolite Materials and Catalysis

Catalysis Research
2024, volume 4, issue 1
doi:10.21926/cr.2401002

Received: October 24, 2023
Accepted: December 26, 2023
Published: January 28, 2024

Abstract

The research describes a sustainable approach for the synthesis of zeolite NaA using kaolin as an alternative source of silica. The main objective of this research was to prepare NaA zeolite using metakaolin derived from kaolin from the state of Rio Grande do Norte, Brazil, as an alternative source of silica, reducing the production cost and evaluating its thermal stability. In addition, a study of the thermal stability of the zeolite and cost estimates for zeolite production were carried out. Traditional methods of zeolite synthesis, mainly through hydrothermal processes, are often associated with high costs, waste generation, and negative environmental impacts. This work addresses these concerns by exploring a more sustainable approach. The kaolin used in the study was characterized by X-ray diffraction, energy-dispersive X-ray fluorescence spectroscopy, infrared spectroscopy, and thermogravimetry. These techniques help confirm the composition and properties of the raw material. NaA zeolite was synthesized by replacing sodium silicate with metakaolin using the hydrothermal synthesis method. The NaA zeolite was characterized by XRD and IR, which helped verify its purity and structural order. The study's results demonstrated that kaolin waste mainly consists of kaolinite, which suggests that it can be effectively used as a source of silica. Furthermore, the research successfully produced low-cost NaA zeolite in a relatively short

synthesis time, achieving high purity and structural order. The study highlights the potential of using kaolin waste as a sustainable source of silica for zeolite production, helping to minimize environmental impacts and reduce processing costs compared to traditional methods. This work presents a promising and sustainable method for producing NaA zeolite from kaolin waste, which has the potential to contribute to cost reduction, waste reduction, and improved environmental sustainability in zeolite production processes. This research is aligned with the broader goals of reducing the ecological footprint of industrial processes while maintaining product quality and efficiency.

Keywords
NaA zeolite synthesis; kaolin; metakaolin; hydrothermal method; low cost; sustainability

1. Introduction

Zeolites are crystalline aluminosilicates of $[SiO_4]^{4-}$ and $[AlO_4]^{5-}$ tetrahedra, forming a well-defined three-dimensional structure. The orientation of the $[SiO4]^{4-}$ and $[AlO_4]^{5-}$ tetrahedra generates pores and channels with molecular dimensions. The excess negative charges produced by Al^{3+} are compensated with alkaline ions (Na^+, K^+…) or alkaline earth metals (Ca^{2+}, Mg^{2+}) surrounded by water molecules located in the space [1].

Synthetic zeolites have seen the identification of over 200 species to date [2]. The applications of synthetic zeolites span diverse fields, from environmental protection (for example, as soil-improving additives and as adsorbents in water and gas purification systems) to medicinal uses [3-6].

Several preparation routes have been highlighted in the literature [7-9]. Moreover, numerous efforts have been dedicated to investigating a range of raw material sources to obtain a versatile zeolite. However, the crucial determinant continues to be the suitable alumina and silica content in the raw materials.

Numerous natural aluminosilicate sources exist, including materials like clay [10-14]. Kaolin, characterized by its low concentration of iron impurities, exhibits a white color due to its main component, kaolinite, possessing an approximate composition of $Al_2Si_2(OH)_4$, with any additional compounds indicating impurities or adsorbed substances [15]. In its natural state, kaolinite lacks reactivity for zeolite crystallization, necessitating activation before synthesis. This activation involves calcination at temperatures exceeding 550°C, leading to structural water removal and metakaolin formation [15].

According to authors [15], as the temperature increases, the meta kaolinite structure collapses, producing a pseudo-amorphous material, the precursor of mullite, where the Al atoms mostly have octahedral coordination. The sample with high levels of Al becomes highly reactive in the synthesis of microporous materials because the zeolite structure consists of Si and Al tetrahedra [16].

There are several methods to synthesize zeolites: hydrothermal, microwave, and steam; however, hydrothermal synthesis is the most promising method and is frequently used. Hydrothermally synthesized zeolite is a multiphase reaction-crystallization process, commonly involving at least one liquid phase and amorphous and crystalline solid phases [17, 18].

Years ago, the attention surrounding the synthesis and application of zeolites obtained from kaolin intensified, driven by their capacity to tackle environmental issues and endorse sustainable practices aligned with the circular economy concept. The synthesis of NaA zeolite from clay minerals continues to be very attractive due to its low cost, thus contributing to the preservation of the environment. In this sense, the synthesis of NaA zeolite using two different routes: (1) conventional hydrothermal, where the silica source was sodium metasilicate, and (2) green route hydrothermal reaction from metakaolin as the silica source was investigated. Furthermore, thermal stability tests were carried out in a muffle furnace in the temperature range of 200 to 600°C for 1 h to evaluate the structural resistance of the NaA zeolite. An estimate of the costs of producing NaA zeolite on a laboratory scale was also carried out.

2. Materials and Methods

All chemicals were purchased from commercial suppliers and used as received, including sodium hydroxide (NaOH – Merck), sodium aluminate ($NaAlO_2$ – Reagen), and Sodium Silicate (Vetec). Kaolin was collected in a local area, Caiçara, Rio Grande do Norte, Brazil.

2.1 Thermal Activation of Kaolin

Metakaolin was produced by calcining kaolin, with a non-crystalline phase, much more reactive than kaolin (Figure 1). The raw material was initially passed through a 200 mesh sieve and dried for 24 h at 110°C, using a circulating air oven to remove moisture. The kaolin was weighed into ceramic crucibles using a semi-analytical balance. Then, the material was placed in a calcination muffle furnace at 700°C for 2 h at 10°C/min. Calcination was carried out to promote the dehydration of kaolinite with the release of water in the form of steam and, therefore, the obtaining of metakaolin. After 2 h, the material was removed from the muffle furnace and cooled in a desiccator [19]. The dehydroxylation reaction can be represented by Equation 1:

$$\boldsymbol{Al_2Si_2O_5(OH)_4 \rightarrow Al_2Si_2O_7 + 2H_2O} \qquad \text{(Eq. 1)}$$

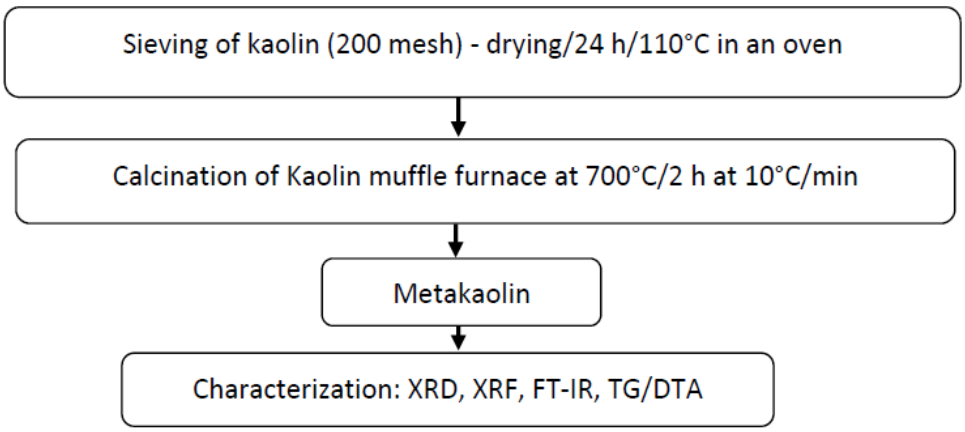

Figure 1 Diagram of the thermal activation of kaolin.

2.2 Syntheses of NaA Zeolite: Conventional Route and Green Route

The steps to be followed in synthesizing conventional NaA zeolite are shown in the diagram in Figure 2. NaA zeolite was synthesized using the synthesis method adopted by the authors [20].

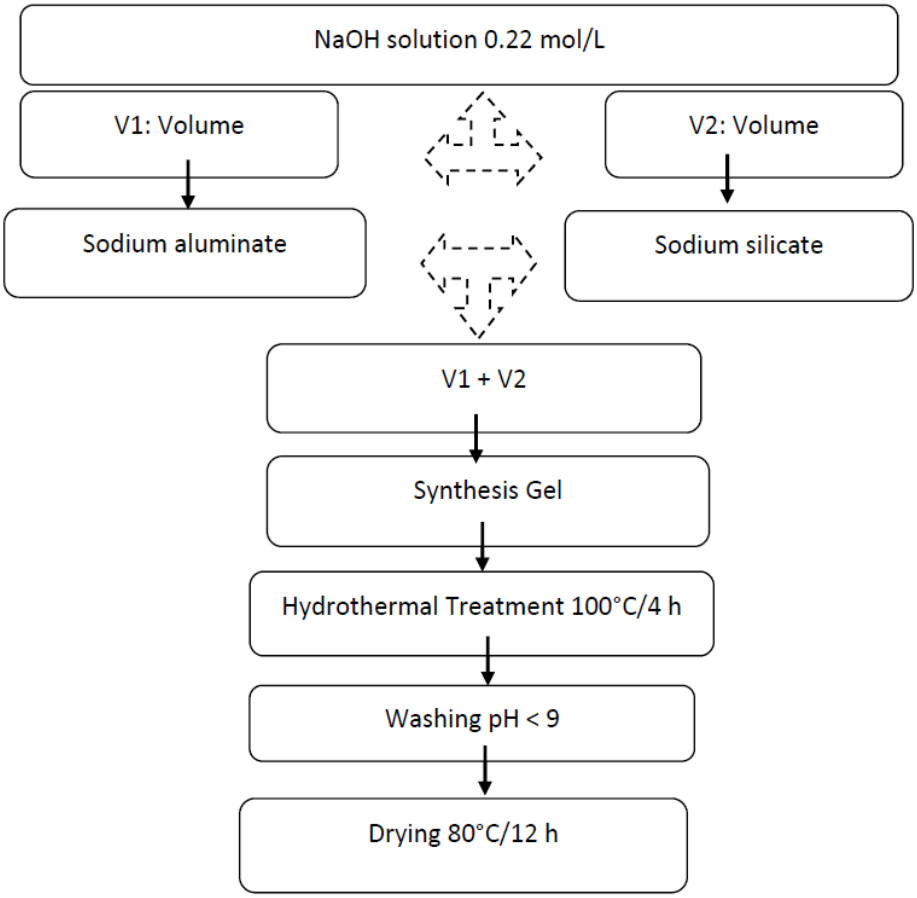

Figure 2 Diagram for synthesis conventional route.

A NaOH solution was prepared: 80 ml of water + 0.723 g of sodium hydroxide, mixed until NaOH was completely dissolved. The sodium hydroxide solution was divided into two equal volumes (V1 and V2) in polypropylene bottles. In the first fraction, V1, 8.258 g of sodium aluminate was added and mixed in a closed bottle until a transparent solution was obtained at room temperature for 10 to 20 min. In the second fraction, V2, 15.48 g of sodium silicate was added and mixed in a closed bottle for 10 to 20 minutes at room temperature. After homogenizing fractions V1 and V2, the sodium silicate solution was quickly poured into the sodium aluminate solution. The system was kept under stirring for approximately 15 minutes until a gel formed at room temperature. The gel formed was transferred to Teflon-coated stainless steel autoclaves with a capacity of 60 mL. Crystallization occurred in static mode in an air circulation greenhouse at 100°C and autogenous pressure. The crystallization time to form the zeolite NaA phase was 4 h. The product was cooled to 30°C, and washed with deionized water until the pH of the filtrate was below 9. This procedure aims to recover the solids. After filtering, the product was dried in an oven at 80°C for 12 h [20].

The final product was named conventional NaA zeolite.

The objective of minimizing operational expenses in the production of zeolite NaA led to the utilization of kaolinite clays for its synthesis. The hydrothermal synthesis procedure adhered to the IZA standard, with a notable departure being the substitution of sodium silicate and sodium aluminate with metakaolin in the synthesis process [21].

The steps to be followed in synthesizing NaA zeolite through alternative sources (Metakaolin) are shown in the diagram in Figure 3.

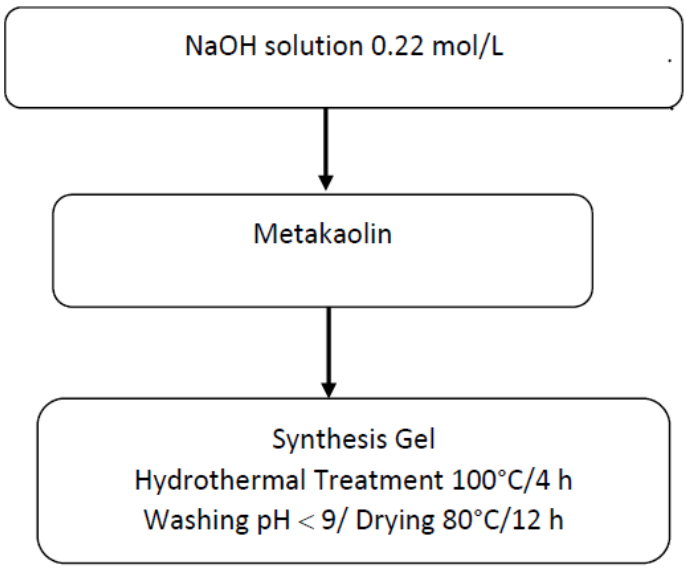

Figure 3 Diagram for the synthesis of the green route.

The final product was named low-cost NaA zeolite.

2.3 Characterization

X-ray diffraction patterns were obtained on a Shimadzu XRD 6000 using Cu Kα radiation at 40 kV/30 mA, with a goniometer velocity of 2°/min and step of 0.02° in the 2θ range from 3.0° to 50.0°.

FT-IR Vertex 70 Model (Bruker) was used to obtain the infrared. The IR spectra were obtained at wavelengths in the 4000-400 cm^{-1} range with a resolution of 4 cm^{-1}.

The X-ray fluorescence spectrometer was the Shimadzu model EDX-720. The generation of X-rays is done through a tube with an Rh target.

The thermogravimetric (TG) and thermal differential (DTA) curves were obtained using equipment model DTG-60H from Shimadzu in an air atmosphere at a heating rate of 10°C/min and a maximum temperature of 1000°C.

2.4 Thermal Stability of Zeolite

A study on the thermal stability of NaA zeolite (conventional route) and NaA zeolite (green route) was carried out, aiming to obtain an adequate temperature to carry out the catalyst regeneration process. 2 g of zeolite was weighed on an analytical balance, and placed in porcelain crucibles to be subjected to heat treatments at a temperature of 200, 300, 400, 500 and 600°C, in a muffle furnace, with a heating rate of 5°C/min for 1 h. Subsequently, the crucibles were removed from the muffle and taken to the desiccator until thermal equilibrium at room temperature.

3. Results and Discussion

3.1 Characterization of the Starting Material

3.1.1 Chemical Analysis

The chemical composition of natural kaolin and thermally activated kaolin (metakaolin) are presented in Table 1.

Table 1 Chemical composition of kaolin and metakaolin.

	Samples	
Oxides (%)	**Natural kaolin**	**Metakaolin**
SiO_2	50.25	50.79
Al_2O_3	47.62	48.55
MgO	0.70	-
K_2O	0.70	0.41
Fe_2O_3	0.34	0.13
SO_3	0.13	-
P_2O_5	0.09	-

Results show that the thermal activation process managed to reduce the number of impurities present in the kaolin, either by eliminating them, such as sulfur trioxide, magnesium oxide, and phosphorus pentoxide, or by lowering their percentage. Quantity, such as ferric oxide and potassium oxide. It is also possible to observe that the samples contain small amounts of iron oxide, which decreased by around 61.00% after the kaolin was subjected to heat treatment. According to the literature, the low percentage of this element in the composition of kaolin is ideal for the synthesis of zeolites. Meanwhile, the amount of silicon dioxide and aluminum oxide had little change in composition. The main elemental components of kaolin and metakaolin are silica and alumina; kaolin has a percentage of SiO_2 higher than the percentage of Al_2O_3, whose SiO_2/Al_2O_3 ratio is close to 1, similar to the value of the SiO_2/Al_2O_3 molar ratio of NaA zeolite. Therefore, metakaolin is the ideal source of Si and Al for synthesizing zeolite NaA [22].

3.1.2 Structural Analysis

XRD was used to verify the crystal structures of the synthesized samples. Figure 4 shows the XRD patterns of the prepared samples.

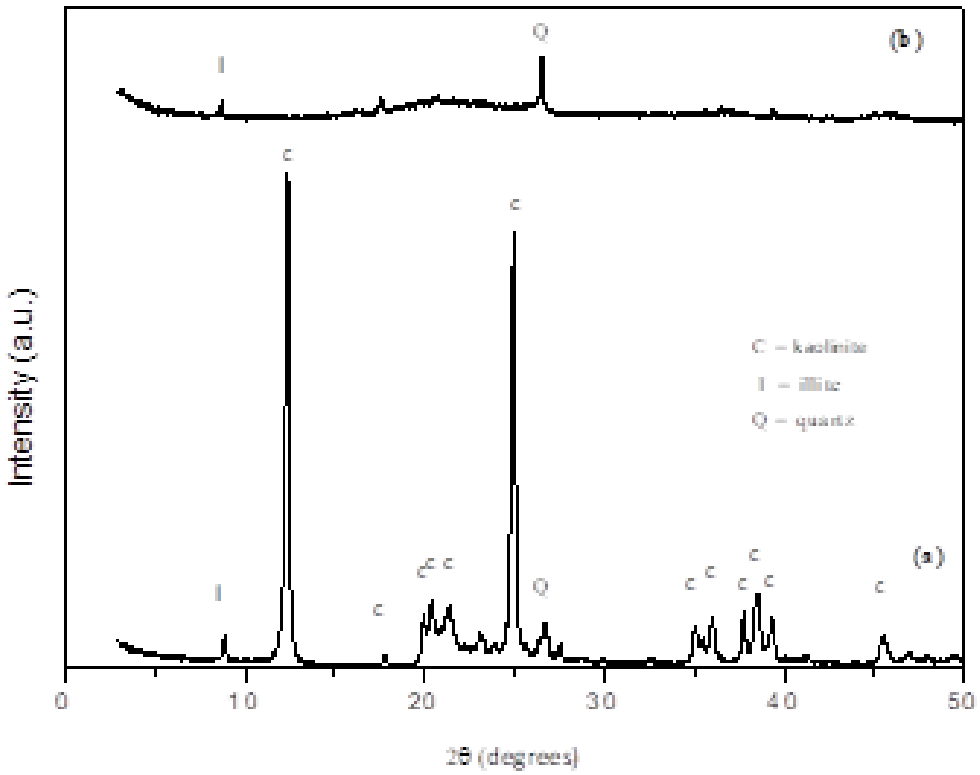

Figure 4 XRD patterns of kaolin and metakaolin**.**

The diffractogram in Figure 4 (a) and (b) shows the XRD results of natural kaolin and thermally activated kaolin (metakaolin), respectively. It is observed that kaolin (Figure 4a) essentially consists of kaolinite mineral clay. The presence of kaolinite in kaolin was confirmed by characteristic reflections at 2θ = 12.41, 20.21 (multiple reflections), and 25.49°, the first and last intense and well-defined [23]. Other clay minerals such as quartz (SiO_2 - JCPDFWIN ICDD 87-2096) and illite ($KAl_2Si_3AlO_{10}(OH)_2$ - JCPDFWIN ICDD 02-0056) are also observed, but with less intense peaks when compared to kaolinite peaks. The small reflection at 2θ 26.5° showed the presence of traces of quartz and 8.86° of illite. After heat treatment at 700°C/2 h, kaolin was transformed into metakaolin (Figure 4b), caused by the collapse of the crystalline structure of kaolin due to the dehydroxylation process. Peaks remaining after calcination, which correspond to quartz and illite, are still observed, as destroying the structure of these clay minerals would require temperatures above 700°C. A large curvature of around 20° in 2θ confirmed the presence of amorphous material. The conversion of kaolinite to metakaolin is approved by the absence of kaolinite diffraction peaks, accompanied by the appearance of amorphous aluminosilicate [22]. Metakaolin is an amorphous material, and the highest diffraction peaks correspond to the presence of quartz (SiO_2), which is the crystalline phase, in metakaolin.

Thermal activation is essential for Kaolin to become reactive in the reaction mixture. This activation is promptly accomplished through calcination, supplying the necessary energy to induce crucial alterations in thermodynamic conditions. This activation process leads to significant modifications in the structure of kaolin, causing a loss of its crystallinity [21].

3.1.3 Thermoanalysis

Figure 5 (a) and 5 (b) show the thermogravimetric (TG) and differential thermal analysis (DTA) curves of kaolin and metakaolin, respectively, using a temperature range of 0-1000°C and a heating rate of 12.5°C/min.

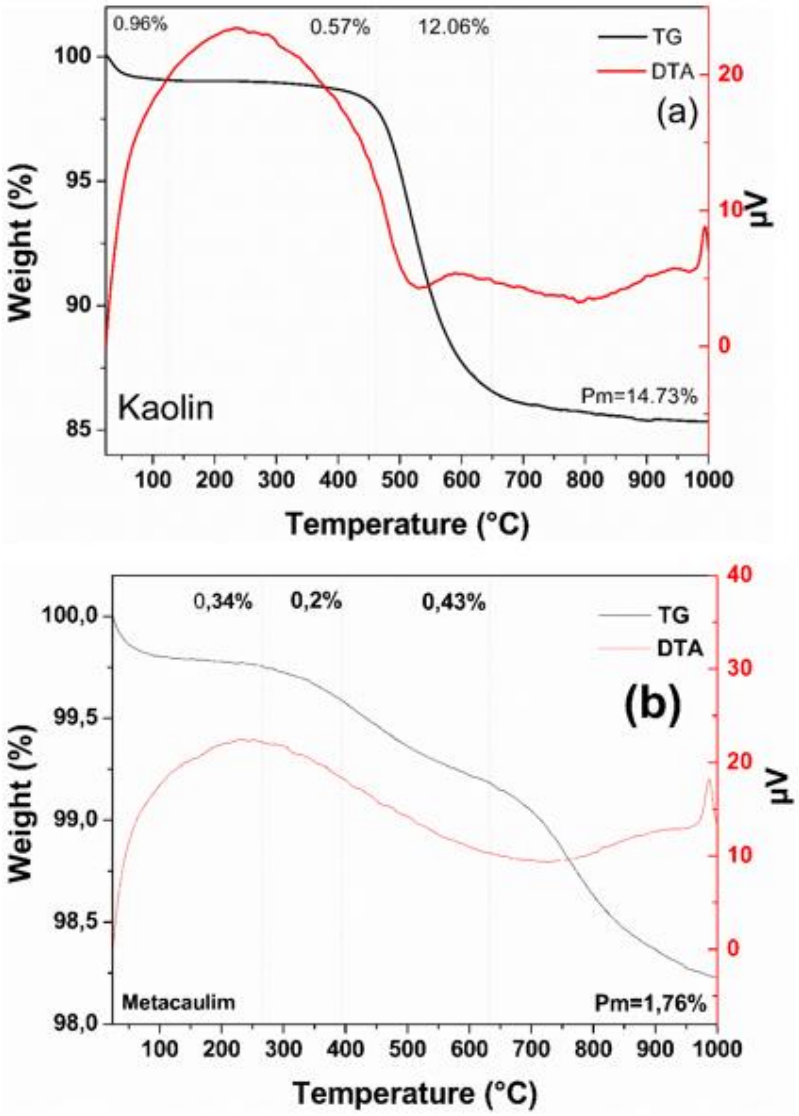

Figure 5 Thermogravimetric (TG) and thermal differential (DTA) curves of kaolin (a) and metakaolin (b).

Analyzing the differential thermal analysis curves [Figure 5a] for kaolin, a slight mass loss of 0.96% is observed in the temperature range of 50-200°C, which is associated with free and adsorbed water loss. Then, a second peak, which corresponds to the most extensive mass loss recorded in the temperature range of 438-666°C with the peak temperature at 535°C; this peak represents a mass loss of 12.06% and corresponds to the dehydroxylation of kaolinite, which can be called the transformation of kaolin into metakaolinite; this process occurs in the temperature range of 500-600°C [24]. Finally, an exothermic peak, around 993°C, indicates the beginning of mullite nucleation.

Finally, in the thermogravimetric analysis, a total mass loss of 14.73% can be observed, corresponding to the losses of organic matter, water, and hydroxyls, confirmed by all the events highlighted in the differential thermal analysis. Analyzing the sample results, it was possible to observe very similar thermograms with a characteristic curve profile following citations found in the literature [25]. When analyzing the metakaolin curve [Figure 5b], mass loss is observed with increasing temperature. However, the rate of mass loss is not constant. As for the energy involved in the process (DTA), the results show three events. The first event is in the temperature range of 100-190°C and is related to the release of free water; the second event is presented in the temperature range of 200-800°C, which is associated with the decomposition of phases with a high carbon content (organic matter), and the presence of water adsorbed in the sample. The third and final event is the presence of the characteristic peak of mullite nucleation at around 990°C. Finally, in the thermogravimetric analysis, a total mass loss of 14.73% for kaolin and 1.76% for metakaolin can be observed, corresponding to the losses of organic matter, water, and hydroxyls, being confirmed by all events highlighted in the differential thermal analysis. Analyzing the sample results, it was possible to observe very similar thermograms with a characteristic curve profile following citations found in the literature [23].

3.2 Characterization of NaA Zeolite

3.2.1 Structural Analysis

Figure 6 (a) and (b) present the results of X-ray diffraction analyses, with a 2θ scan from 3 to 50°, referring to NaA zeolite (conventional route) and low-cost NaA zeolite (green route), obtained by the hydrothermal synthesis method.

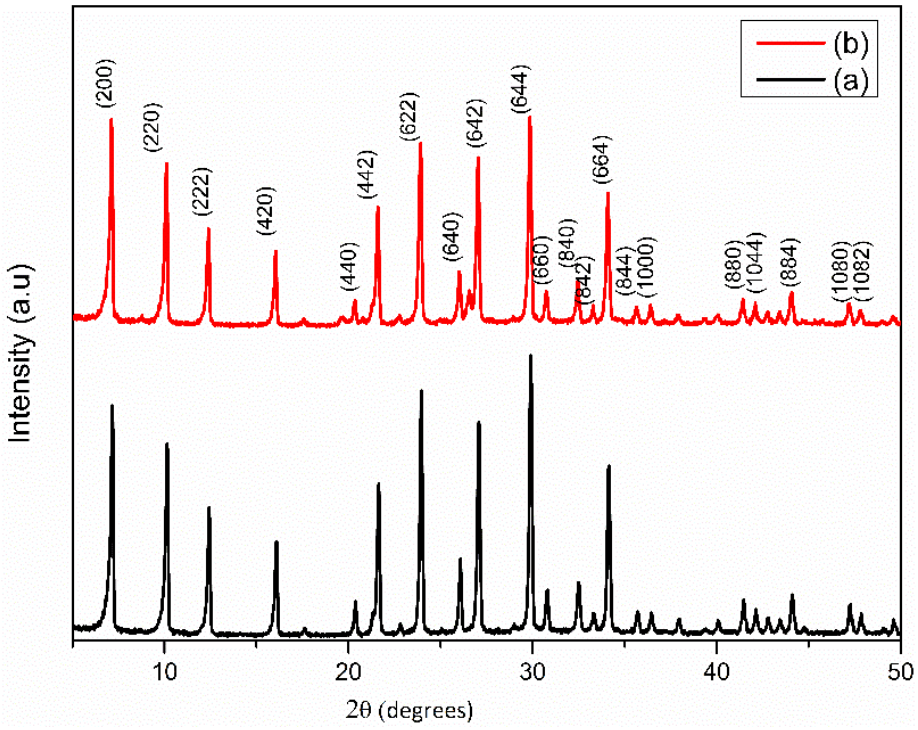

Figure 6 X-ray diffraction patterns of conventional NaA zeolite (a) low-cost NaA zeolite (b).

From the diffractogram presented in Figure 6 (a) and (b), it is observed that the materials obtained have peaks characteristic of zeolite NaA, with peaks corresponding to 2θ values at 7.2, 10.1, 12.5, 16.1, 21.7, 24, 27.1, 29.9 and 34.2, identified by (A), which are typical peaks of sodium zeolite A (NaA) JCPDS 39-222. The results of both diffractograms follow the literature [26], whose characteristics correspond to crystalline materials. Without secondary phases, it has intense and well-defined peaks indicating good crystallinity of the product formed [27].

Figure 6 (b) shows the XRD pattern of the reaction product obtained from the thermally activated kaolin sample. NaA zeolite was accepted as the dominant phase. Only NaA zeolite was synthesized, and the characteristic peaks of this zeolitic material are well delineated, indicating that all the metakaolin had reacted, which shows that it is an excellent starting material [28].

This standard sample was used as a reference for calculating relative crystallinity from Equation 2.

$$\% \text{ Crystallinity } = \frac{\sum Low - cost\ NaA\ zeolite\ peak\ area}{\sum Conventional\ NaA\ zeolite\ peak\ area} \quad (\text{Eq. } 2)$$

Table 2 presents the crystallinity results of conventional NaA zeolite and low-cost NaA zeolite.

Table 2 Crystallinity of samples.

Zeolite NaA	Relative Crystallinity by XRD (%)	*Average crystal size by XRD (nm)	Formed phase
Conventional	100	55.5	NaA
Low-cost	89	50.9	NaA

***from Scherrer Equation**

The relative crystallinity of conventional NaA zeolite and low-cost NaA zeolite was found to be 100% and 91%, respectively. The findings outlined in Table 2 reveal satisfactory crystallinity levels exceeding 90% for both samples. This observation signifies a notable degree of molecular and structural ordering in pure reagents, affirming the efficacy of the synthesis using alternative reagents. Consequently, alternative reagents like metakaolin, derived from kaolin, are suitable for crafting materials characterized by a high degree of crystallinity at a cost-effective aggregate.

The average crystal size of conventional NaA zeolite and low-cost NaA zeolite was 55.5 and 50.9 nm, respectively.

3.2.2 FTIR Measurements

Figure 7 shows the FTIR spectra of kaolin and metakaolin (a), conventional NaA zeolite, and low-cost NaA zeolite (b).

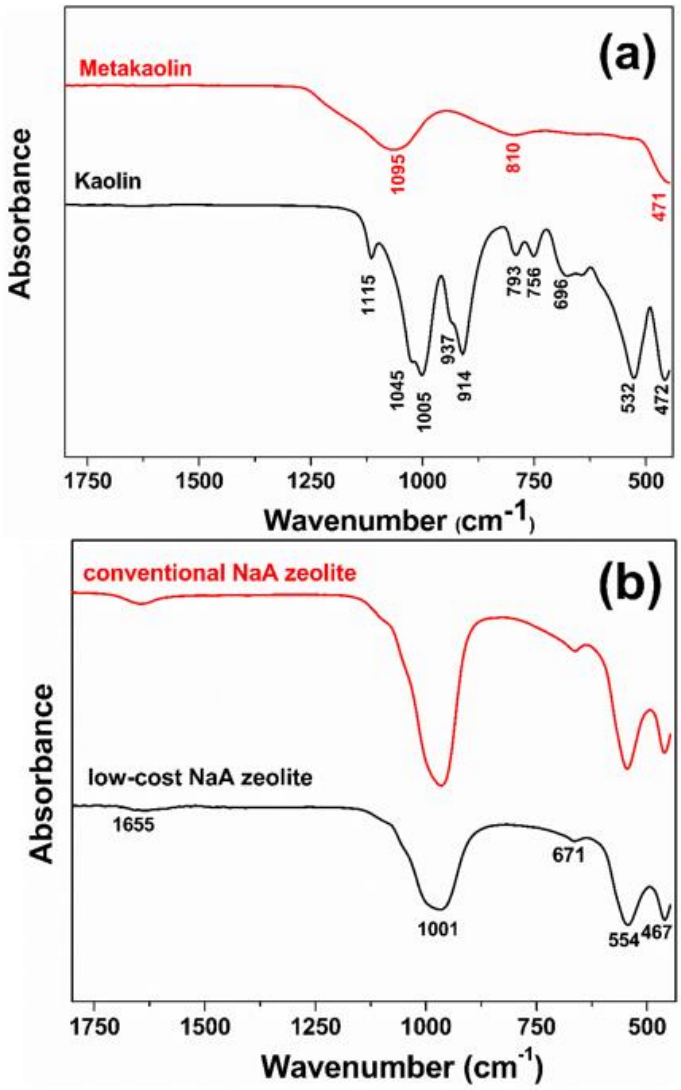

Figure 7 FTIR spectra of kaolin and metakaolin (a) and conventional NaA zeolite and low-cost NaA zeolite (b).

The transformation of kaolin to metakaolin and then to zeolite A can be observed from IR spectra in Figure 7 (a) in the lattice region (1400-400 cm^{-1}). The kaolin starting material gives at least well-defined IR bands in this region due to Si–O, Si–O–Al, and Al–OH vibrations. The conversion to metakaolin removes these bands, leaving a broad, intense asymmetric band at 1095 cm^{-1} as the significant feature. The disappearance of the 914 and 937 cm^{-1} bands indicates the loss of Al–OH units, while the changes in Si–O stretching bands and the disappearance of the Si–O–Al bands at 793 and 756 cm^{-1} are consistent with distortion of the tetrahedral and octahedral layers [29].

The FTIR spectra of the two samples (Figure 7b) show the bands at 1001, 671, 554, and 467 cm^{-1} bending vibration, respectively. In the FTIR spectra of the conventional NaA zeolite and at low-cost NaA zeolite in Figure 8 (b), the characteristic bands for zeolite framework at 554 cm^{-1} due to the external vibration of double four-rings, 1001 cm^{-1} for the internal vibration of (Si, Al)–O asymmetric stretching, 671 cm^{-1} for the inner vibration of (Si, Al)–O symmetric stretching, and 467 cm^{-1} for the internal vibration of (Si, Al)–O bending were observed. The OH-related band also appeared at about 1655 cm^{-1} [30]. These results indicate the high purity and crystallinity of the synthesized NaA zeolite.

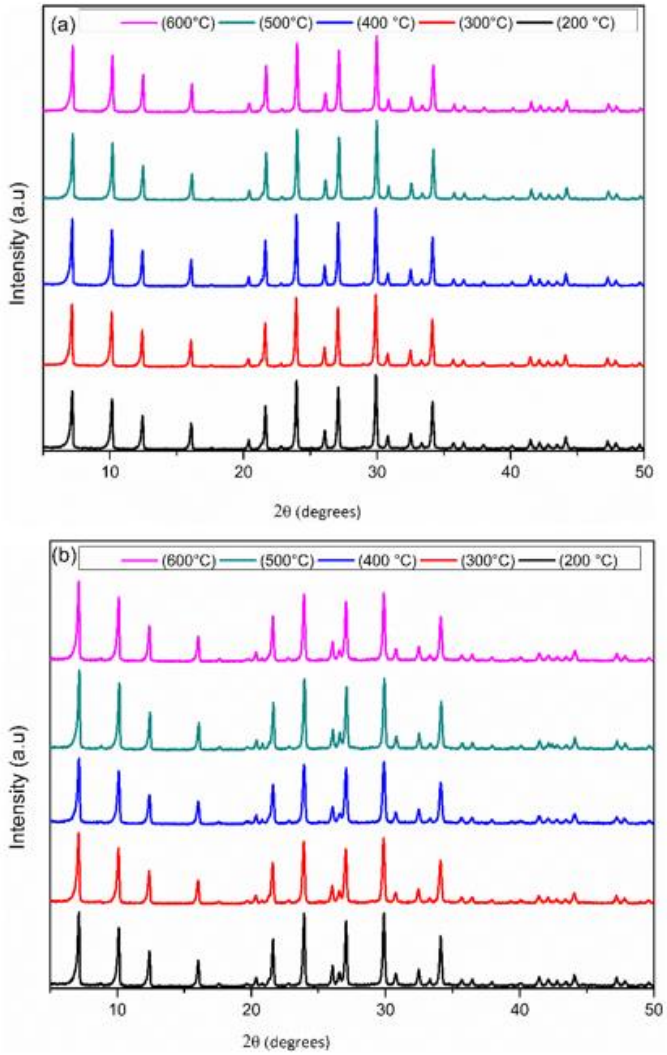

Figure 8 X-ray diffraction pattern of conventional NaA zeolite (a) and low-cost NaA zeolite (b) after thermal treatment at 200, 300, 400, 500, and 600°C.

3.3 Study of Thermal Stability of NaA Zeolite

Typically, zeolites find extensive application in industrial settings that involve high-temperature conditions. Specifically, they serve as sorbents under elevated temperatures. Consequently, the thermal stability of zeolites emerges as a crucial characteristic. The thermal treatment induces a structural transformation in zeolites, leading to the collapse into intermediate amorphous phases. Subsequently, a recrystallization process gives rise to another crystalline phase.

A beneficial technique to study the thermal stability of zeolite is in situ X-ray diffraction. The XRD patterns of NaA zeolite (route conventional and green route) heated in air are shown in Figure 8 (a) and (b).

It can be seen in Figure 8 (a) and (b) that at all temperatures used in the thermal treatment (200 to 600°C), the conventional NaA zeolite and the low-cost NaA zeolite remained as the main constituent, without the presence of secondary phases. At 200°C, the zeolite structure begins a disordering process with a slight decrease in intensity and broadening of its peaks in both samples. From 300°C, the structure becomes ordered again, increasing the intensity of its peaks with

increasing temperature [30]. As can be seen in Figure 8, among the temperatures tested, the most appropriate for use in thermal regeneration is the temperature of 600°C since it is in this temperature range that the structure of the zeolite appears more ordered and with greater intensity.

Table 3 presents the crystallinity and average crystal size results of conventional NaA zeolite after heat treatment.

Table 3 Crystallinity and average crystal size of conventional zeolite NaA.

Conventional zeolite NaA	**200°C**	**300°C**	**400°C**	**500°C**	**600°C**
Relative Crystallinity by XRD (%)	97	98	99	99	98
Average crystal size by XRD (nm)	55.1	54.6	57.2	57.1	58.3

The results of crystallinity and average crystal size for low-cost NaA zeolite following heat treatment are presented in Table 4.

Table 4 Crystallinity and average crystal size of low-cost zeolite NaA**.**

Low-cost zeolite NaA	**200°C**	**300°C**	**400°C**	**500°C**	**600°C**
Relative Crystallinity by XRD (%)	87	89	88	88	88
Average crystal size by XRD (nm)	53.5	47.3	44.8	53.1	51.7

Upon comparing the outcomes of the untreated conventional NaA zeolite (as indicated in Table 2) with those subjected to heat treatment (as detailed in Table 3), it becomes evident that there was minimal fluctuation in crystallinity and average crystal size.

After heat treatment, the low-cost zeolite (as indicated in Table 4) showed no change in crystallinity (as detailed in Table 2), but there was a change in the average crystal size.

Another observation is that heat treatment up to 600°C had no collapse of the conventional zeolite NaA and low-cost zeolite NaA structures. This fact agrees with the authors [31] because the structure of zeolite A should only collapse at temperatures above 900°C.

3.4 Estimation of Raw Material Costs

Table 5 presents the evaluation of cost estimates for the raw materials used to prepare conventional NaA zeolite and low-cost NaA zeolite.

Table 5 Cost estimates for obtaining 10 g of samples.

		conventional zeolite	**low-cost zeolite**
Material	raw material value (Kg)	Raw material value to obtain 10 g	Raw material value to obtain 10 g
Sodium Hydroxide (R$)	60.00	0.04	0.04
Sodium aluminate (R$)	502.40	4.15	-
Sodium silicate (R$)	200.00	3.10	-
Kaolin (R$)	0.85	-	0.0085
Total raw material cost (R$)		7.29	0.0485

It takes 7.29 reais to produce 10 g of conventional zeolite NaA and 0.0485 reais to produce low-cost zeolite NaA. These values do not take energy costs into account.

Table 6 presents the energy cost estimates for producing conventional NaA zeolite and low-cost NaA zeolite.

Table 6 Energy cost estimates for obtaining 10 g of samples.

Equipment	Power (Kw/h)	Usage time (h)	Tariff (R$/Kw/h)	**Cost energetic conventional (R$)	Cost energetic low-cost (R$)
***Stove**	0.82	4 (synthesis) 24 (drying) 12 (drying after synthesis)	0.48605	1.59 - 4.78	1.59 0.50 4.78
filter, vacuum pump					
muffle furnace	6.00	3:10		-	0.48
Total energy cost (R$)				6.37	7.35

*Stove = drying + synthesis + drying after synthesis

** Cost energetic conventional without ICMS (Tax on Circulation of Goods and Services)

To produce low-cost zeolite NaA, it is necessary to consider the energy cost of kaolin sintering. 240 g of kaolin was used in oven drying and muffle burning, and 200 g of metakaolin was obtained. To calculate the energy cost, it is necessary to consider that to get 10 g of NAa zeolite, 10.50 g of metakaolin is needed, so the calculation in the Table above was carried out based on this analysis.

The total cost was estimated based on the price of raw materials and the energy cost for the drying, sintering, washing, filtration, and production process.

The projected energy expense for producing 10 g of conventional NaA zeolite amounted to 6.37 reais, whereas the estimated cost for obtaining the same zeolite was 7.35.

Hence, the overall expenditure for manufacturing 10 g of conventional NaA zeolite is 13.66 reais, encompassing both the raw material cost (as detailed in Table 5) and the energy cost (as specified in Table 6).

Thus, the comprehensive expense for generating 10 g of economical zeolite NaA is 7.39, reflecting the combined estimate of raw material (as indicated in Table 5) and energy costs (as presented in Table 6).

Upon comparing the total costs of the two zeolites, it becomes evident that the overall cost of the economical NaA zeolite was lower than that of the conventional NaA zeolite.

This study assessed the expenses associated with bulk raw materials by utilizing pricing information gathered from vendor websites.

The manufacturing cost estimate for the synthesis of zeolite A was carried out on a laboratory-scale synthesis.

4. Conclusions

The considerable potential of Brazilian kaolin as a raw material for synthesizing zeolite NaA stems from its Si/Al ratio, which closely approaches one. Thermal treatment is essential to activate the

kaolin, transforming the crystalline phase of kaolinite into amorphous metakaolin. A 2-hour calcination at 700°C effectively yields amorphous metakaolin with a SiO_2/Al_2O_3 content ratio 1.05.

Zeolite A could be efficiently synthesized from metakaolin by using a green route.

One of the goals of this investigation was to acquire more comprehensive structural insights into zeolite A. In this study, we scrutinized the thermal behavior of zeolite A using XRD, analyzing the results of its structural characteristics. Our findings led us to the conclusion that there was no discernible change in crystallinity up to 600°C.

The results of production cost estimation for 10 g of NaA zeolite (green route) were compared with those for NaA zeolite (conventional route). The observations revealed that the cost of the low-cost zeolite NaA is less than that of the traditional zeolite NaA.

Acknowledgments

The authors gratefully acknowledge to the Coordenação de Aperfeiçoamento de Pessoal de Nível Superior (CAPES) for the financial support. We thank Laboratory of Multifunctional Materials and Nanocomposites LAMMEN-ECT UFRN for the FTIR analysis.

Author Contributions

Antusia dos Santos Barbosa: Investigation, Formal analysis, Writing – Original Draft; Meiry G. F. Rodrigues: Conceptualization, Formal analysis, Funding acquisition, Writing – Review & Editing.

Funding

Coordenação de Aperfeiçoamento de Pessoal de Nível Superior (CAPES).

Competing Interests

The authors have declared that no competing interests exist.

References

1. Breck DW. Zeolite molecular sieves: Structure, chemistry and use. New York, NY, USA: John Wiley &Sons Inc.; 1974.
2. Zhao Y, Zhang B, Zhang X, Wang J, Liu J, Chen R. Preparation of highly ordered cubic NaA zeolite from halloysite mineral for adsorption of ammonium ions. J Hazard Mater. 2010; 178: 658-664.
3. Li Y, Li L, Yu J. Applications of zeolites in sustainable chemistry. Chem. 2017; 3: 928-949.
4. Szerement J, Kloc AS, Jarosz R, Bajda T, Hersztek MM. Contemporary applications of natural and synthetic zeolites from fly ash in agriculture and environmental protection. J Clean Prod. 2021; 311: 127461.
5. El-Nahas S, Osman AI, Arafat AS, Al-Muhtaseb AH, Salman HM. Facile and affordable synthetic route of nano powder zeolite and its application in fast softening of water hardness. J Water Process Eng. 2020; 33: 101104.
6. Osman AI, El-Monaem EM, Elgarahy AM, Aniagor CO, Hosny M, Farghali M, et al. Methods to prepare biosorbents and magnetic sorbents for water treatment: A review. Environ Chem Lett. 2023; 21: 2337-2398.

7. Jin Y, Li L, Liu Z, Zhu S, Wang D. Synthesis and characterization of low-cost zeolite NaA from coal gangue by hydrothermal method. Adv Powder Technol. 2021; 32: 791-801.
8. Gadina JM, Afolabi EA, Kovo AS, Abdulkareem AS, James MO. A retrospect on recent research works in the preparation of zeolites catalyst from kaolin for biodiesel production. Biofuels. 2023; 14: 315-332.
9. Tanwongwan W, Chollacoop N, Faungnawakij K, Assabumrungrat S, Nakhanivej P, Eiad-Ua A. Combination of natural silica and alumina sources for synthesis of MCM-22 zeolite. Heliyon. 2023; 9: e18772.
10. Ayele L, Pérez-Pariente J, Chebude Y, Díaz I. Conventional versus alkali fusion synthesis of zeolite A from low grade kaolin. Appl Clay Sci. 2016; 132; 485-490.
11. Wang JQ, Huang YX, Pan Y, Mi JX. Hydrothermal synthesis of high purity zeolite A from natural kaolin without calcination. Microporous Mesoporous Mater. 2014; 199: 50-56.
12. Pereira PM, Ferreira BF, Oliveira NP, Nassar EJ, Ciuffi KJ, Vicente MA, et al. Synthesis of zeolite A from metakaolin and its application in the adsorption of cationic dyes. Appl Sci. 2018; 8: 608.
13. Wang P, Sun Q, Zhang Y, Cao J. Synthesis of zeolite 4A from kaolin and its adsorption equilibrium of carbon dioxide. Materials. 2019; 12: 1536.
14. Belviso C, Cavalcante F, Lettino A, Fiore S. A and X-type zeolites synthesised from kaolinite at low temperature. Appl Clay Sci. 2013; 80: 162-168.
15. Murray HH. Traditional and new applications for kaolin, smectite and palygorskite: A general overview. Appl Clay Sci. 2000; 17: 207-221.
16. Ross CS, Kerr PF. The Kaolin minerals[1]. J Am Ceram Soc. 1930; 13: 151-160.
17. Cundy CS, Cox PA. The hydrothermal synthesis of zeolites: Precursors, intermediates and reaction mechanism. Microporous Mesoporous Mater. 2005; 82: 1-78.
18. Liu H, Peng S, Shu L, Chen T, Bao T, Frost RL. Magnetic zeolite NaA: Synthesis, characterization based on metakaolin and its application for the removal of Cu^{2+}, Pb^{2+}. Chemosphere. 2013; 91: 1539-1546.
19. Barbosa AS, Araujo ME, Rodrigues MG. Synthesis of zeolite NaA using low cost material and application as adsorbent in the removal of crystal violet dye. Conjecturas. 2022; 22: 168-180.
20. Thompson RW, Huber MJ. Analysis of the growth of molecular sieve zeolite NaA in a batch precipitation system. J Cryst Growth. 1982; 56: 711-722.
21. Loiola AR, Andrade JC, Sasaki JM, Da Silva LR. Structural analysis of zeolite NaA synthesized by a cost-effective hydrothermal method using kaolin and its use as water softener. J Colloid Interface Sci. 2012; 367: 34-39.
22. Liu J, Huang X, Zhao K, Zhu Z, Zhu X, An L. Effect of reinforcement particle size on quasistatic and dynamic mechanical properties of Al-Al_2O_3 composites. J Alloys Compd. 2019; 797: 1367-1371.
23. Khan MI, Khan HU, Azizli K, Sufian S, Man Z, Siyal AA, et al. The pyrolysis kinetics of the conversion of Malaysian kaolin to metakaolin. Appl Clay Sci. 2017; 146: 152-161.
24. Rashad AM. Alkali-activated metakaolin: A short guide for civil engineer–An overview. Constr Build Mater. 2013; 41: 751-765.
25. Moore DM, Reynolds RC. X-ray diffraction and the identification and analysis of clay minerals. Oxford, UK: Oxford University Press; 1989.

26. Achiou B, Beqqour D, Elomari H, Bouazizi A, Ouammou M, Bouhria M, et al. Preparation of inexpensive NaA zeolite membrane on pozzolan support at low temperature for dehydration of alcohol solutions. J Environ Chem Eng. 2018; 6: 4429-4437.
27. Treacy MM, Higgins JB. Collection of simulated XRD powder patterns for zeolites. 4th ed. Amsterdam: Elsevier; 2001.
28. Maia AA, Dias RN, Angélica RS, Neves RF. Influence of an aging step on the synthesis of zeolite NaA from Brazilian Amazon kaolin waste. J Mater Res Technol. 2019; 8: 2924-2929.
29. Maia AA, Angélica RS, Neves RF. Thermal stability of the zeolite A synthesized after kaolin waste from Amazon region. Cerâmica. 2008; 54: 345-350.
30. Chen X, Wang Y, Wang C, Xu J, Li T, Yue Y, et al. Synthesis of NaA zeolite via the mesoscale reorganization of submolten salt depolymerized kaolin: A mechanistic study. Chem Eng J. 2023; 454: 140243.
31. Kosanovic C, Subotic B, Smit I. Thermally induced phase transformations in cation exchanged zeolites 4A, 13X and synthetic mordenite and their amorphous derivatives obtained by mechanochemical treatment. Thermochim Acta. 1998; 317: 25-37.